Preprints (www.preprints.org) | NOT PEER-REVIEWED | Posted: 19 October 2019 doi:10.20944/preprints201910.0226.v1

Friction Stir Processing Of TIG And Friction Stir Welded Dissimilar Alloy Joints: A Review

S. Mabuwa[1], V. Msomi[1]

Cape Peninsula University of Technology (South Africa)

Abstract

The use of aluminium alloys continues to grow in many applications to mention a few aerospace, automotive, electronics, electricity, construction and food packaging. With so much demand there is a new interest in welding of dissimilar aluminium alloys. Some of the welding techniques used to join dissimilar aluminium alloys include friction stir welding and TIG welding. The welding of dissimilar alloys affects the mechanical properties negatively due to porosity and cracking during the welding. This then suggests that there should be a process which can be used to improve the dissimilar alloys mechanical properties post its production. Friction stir processing was found to be one of the mechanical techniques that could be used to improve the mechanical properties of the material. This paper reports on the literature on the friction stir welding, TIG welding and friction stir processing techniques published so far, with the aim to identify the gap in the use of friction stir process as a post processing technique of the weld joints.

KeyWords: *Friction stir welding; TIG welding; Friction stir processing; Dissimilar alloys; Aluminium alloys; Mechanical properties; Microstructure.*

1 Introduction

Aluminium and its alloys are widely used in automotive, aeronautical and food industries because of their low density, high specific strength, good corrosion resistance, good workability, high thermal and electrical conductivity, attractive appearance, and intrinsic recyclability [1], [2]. In order to improve performance while controlling the cost of aluminium alloys in these industries, there is an increasing demand to weld dissimilar aluminium joints [3]. The welding techniques being dealt with being the tungsten inert gas (TIG) welding and friction stir welding (FSW).

The different physical and chemical properties in dissimilar aluminium alloy combinations have been noticed to have an impact on the weld strength due to solidification cracking, porosity, the formation of intermetallic and the likes. For that reason, the post processing of the welded joints using the friction stir processing technique comes highly recommended to strengthen the weld.

Friction stir processing (FSP) is a solid-state technique involving the use of a non-consumable rotating tool to refine and homogenize microstructures in metallic components or metals. It is one of the processes derived from friction stir welding which was initially established by The Welding Institute. FSP uses the same principle as FSW, (see Figure 1) but does not join metals rather modifies the local microstructure in the near-surface layer of metals [4].

Preprints (www.preprints.org) | NOT PEER-REVIEWED | Posted: 19 October 2019 doi:10.20944/preprints201910.0226.v1

FSP works by plunging a specific cylindrical non-consumable tool into the plate and kept stationary for a few seconds. This is done to allow the temperature to stabilize, the rotating tool gets released so that it travels along the surface to be welded. The tool travels from the start to the end of the plates resulting in the attainment of the weld. When the process is finished, the tool is then unplunged, leaving a small hole or rather travels to an offset distance to avoid leaving a hole. The side in which the tangential velocity of the tool surface is parallel to the traverse direction is called the advancing side, and the non-parallel side is called the retreating side [5].

The present review aims to discuss and analyze the available literature on friction stir processing of both similar and dissimilar TIG welded as well as FSW joints.

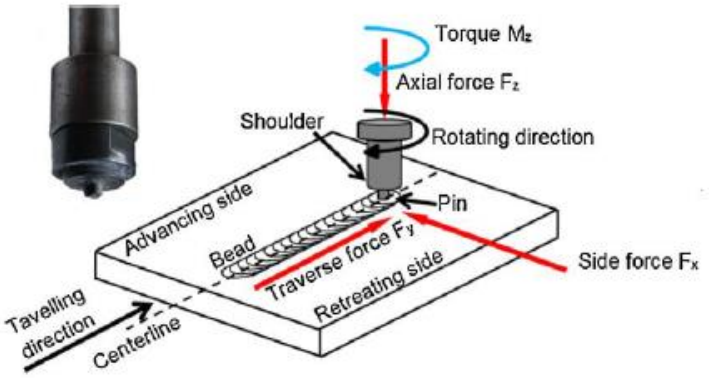

Figure 1: Schematic illustration of FSP method [6].

2.1 Friction Stir Welding of Dissimilar Aluminium Alloys

During the FSW of dissimilar alloys, the hardest material is usually positioned on the advancing side in order to increase the hardness of the weld [7]. Simar et al., [8] found that locating the weakest material (6005A-T6) on the retreating side of a 6005-2017 dissimilar weld favoured stronger dissimilar welds, but this positioning is dependent on the welding conditions.

Aluminium alloy (AA) 2219-T87 was friction stir welded to AA5083-H321 [9]. The tests conducted were the microstructural analysis, hardness, and tensile tests. Microstructural analysis revealed that the nugget region was primarily composed of AA2219, which was placed on the advancing side. The hardness tests revealed that the lowest hardness in the weldment occurred in the HAZ on AA5083 side, where the tensile specimens failed. The joint efficiency of 90% was attained, which was noticeable higher than what can be achieved incase of fusion welding.

Friction stir welding of the 3mm thick AZ31B magnesium alloy and 5052-H aluminium alloys was performed by Taiki et al., [10]. The aluminium plate was positioned on the advancing side and Mg plate on the retreating side. The FSW tool was made of the JIS SKD61 tool steel material. The tool shoulder diameter was 12mm, probe diameter of 4mm and 2.9mm in length. The inclination angle used was 3º with a tool load of 10kN. The welding parameters were the rotational speed range of 800 – 1600rpm and welding speed of 100 - 400mm/min. Tests performed included the microstructural analysis, Vickers hardness tests and tensile tests.

The microstructure analysis revealed grain refinement from 30µm (A5052-H) to 10µm in the FSW joint by dynamic recrystallization. The hardness decreased from 70HV (BM A5052-H) to 60HV in SZ. Hardness distributions of the cross-section revealed that the intermetallic compounds (IMCs) partly existed in stir zone (SZ). The tensile test results showed that all samples of the dissimilar FSW joint broke at the stir zone of AA5052. The ultimate tensile strength (UTS) and elongation of the dissimilar joint were 147MPa and 3.4% respectively. The dissimilar joint efficiency of 61% was achieved between A5052-H and AZ31B.
Cavaliere & Panella, [11] conducted a study on the effect of tool position on the fatigue properties of dissimilar 4mm thick 2024-7075 AA sheets joined by FSW. The welding parameters utilized were the rotational speed of 1600rpm and traverse speed of 120mm/min. AA2024 was situated on the advancing side of the tool and AA7075 was situated on the retreating side. The tests conducted were residual stresses, Vickers hardness, tensile, microstructural analysis and fatigue tests. The highest measured hardness value (190HV) was found in the nugget zone of the material with the tool 1mm far from the weld line, 150HV on the HAZ region with the tool at 1.5mm from the weld line. The maximum tensile properties of 2024-7075 AA joint obtained were the UTS of 460MPa, yield strength of 395MPa and elongation of 4.5%. A ductile behaviour was noticed on the fracture surfaces of the tensile tested specimens characterized by the presence of very fine dimples. The strong effect on fatigue crack growth was attributed to the positive Kr value measured on the cross-section of the different welds.

Peng et al., [12] successfully friction stir welded the 5mm A06-H112 and 6061-T651 aluminium alloys under forced air cooling (FAC) and natural cooling (NC) conditions. AA5A06 was positioned on the advancing side and AA6061 on the retreating side. The pressure of the forced air was 0.5MPa, and the blowing direction was along the welding direction and had an intersection angle of 30° with the surface of the materials. Three different tool rotational speeds of 600, 900, and 1200rpm and two welding traverse speeds of 100 and 200mm/min were applied. Tensile tests, microstructure analysis, nanoindentation hardness test, and tensile fracture analysis were performed. The nanoindentation hardness tests results and microstructure analysis showed that the cooling process can be accelerated using forced air cooling, suppressing the coarsening of grains and the dissolution of precipitate phases, contributing to strengthening and narrowing the weakest area of the joint. The tensile strength of FAC joints was improved by 10% when compared with NC joints. SEM analysis of the tensile fracture surface showed an increase in the number of dimples and reduction of dimple size of the FSW with FAC compared to those of NC.

Upadhyay and Reynolds, [13] investigated the effects of thermal boundary conditions in friction stir welded 6.35mm thick 7050-T7451 high strength aluminium alloy sheets. Welds were made under laboratory air and completely submerged in water conditions. The submerged condition was a mixture of 50% ethylene glycol, 50% water and 13.6kg of dry ice resulting in a steady far-field plate temperature of approximately −25ºC during FSW. The temperature during FSW was recorded using thermocouples spot welded into the probe on the axis of rotation on the probe mid-plane height. Thermocouples were also placed on the HAZ region with a minimum hardness on the advancing side of the weld at the mid-plane height. Weld response variables, hardness distributions, joint strength and nugget grain size were measured and correlated with boundary conditions and welding parameters. In the submerged welds a consistent decrease in the peak temperature

and increase in cooling rate were observed. Submerged welds showed improvement in tensile strength and elongation in comparison to traditional FSW (in the air).

During the FSW of dissimilar alloys intermetallic compounds (IMCs) are formed. IMCs have a brittle nature which could lead to a greater mechanical weakness [14]. FSW also allowed joining of 3mm thick dissimilar AA2024-T3 and AZ31 magnesium alloy [15]. A constant rotational speed of 2500rpm and varying welding speeds (200, 300, 400 and 550mm/min) was used. SEM outfitted with EDS was used to dissect the dissemination of stages in the SZ. The results revealed that on the regions occupied by AA2024, the redistribution of phases in the SZ lower portion was caused by increasing the welding speed, while the AZ31 concentrated the region beneath the tool shoulder. Regardless of the welding speed on the advancing side of AA2024 a laminated structure was formed in the SZ near the boundary between SZ and TMAZ. However, in the HAZ region of the same alloy increasing welding speed had a significant influence on the hardness distribution, but less effective for AZ31 located on the retreating side. The hardness in SZ increased from 65 to 220HV due to the presence of the IMCs. The major difficulty was experienced in controlling the formation of IMCs in the interface between both materials.

AA6061-T6 and AA7050-T7451 were friction stir welded to assess the microstructure and mechanical properties of the dissimilar welded joint. [16]. The welding parameters used included three different tool rotational speeds (270, 340, and 410rpm) and a constant transverse speed of 114mm/min. AA7050-T7451 was positioned on the advancing side and AA6061–T6 was positioned on the retreating side of the tool. Tests conducted included tensile testing, microhardness, microstructural analysis, SEM and EDS. The EDS results confirmed the existence of three distinct layers. Layer 1 and layer 2 consisting of the nominal composition for the AA6061 and AA7050 respectively and layer 3 consisting of a combination of both alloys. Similar results were reported by Gou et al., [17] on dissimilar AA6061-AA7075 FSW. The increase of tool rotational speed resulted in increase in material intermixing and joint strength. During the tensile test, all the specimens fractured on the AA6061 side of the joint on the HAZ due to low tensile strength. However, for the low tool rotational speed, failure occurred in the stir zone due to poor material intermixing. SEM analysis revealed the presence of a large number of dimples indicating the overload and ductile nature of the fracture.

Mofid et al., [18] performed a study on the friction stir welding of the 3mm thick AZ31C-O magnesium alloy to 5083 aluminium alloy in air and under nitrogen liquid. The rotational speed of 400rpm and travel speed of 50mm/min were used. K-type thermometers were embedded on the workpieces. The temperature profile, microstructure, SEM analysis and hardness tests were conducted. In the stir zone of the air-welded specimen, there was a formation of IMCs because of constitutional liquation causing the weld to crack. The stir zone of under liquid nitrogen-welded specimen showed that the formation of IMCs was suppressed significantly because of lower heat input. The XRD analysis results exhibited the intermetallic phases of Al3Mg2, Al12Mg17 and Al2Mg3. The stir zone of the underwater welded specimen showed a smoother interface and less intermixing. The obtained maximum temperature during the welding was 676K and 651K respectively during air weld and under water weld.

Dissimilar aluminium alloys 2024-T365 and 5083-H111 were successfully welded by friction stir welding process [19]. Varying process parameters were employed to analyse the influence of microstructure and tensile properties. The combination of the highest speeds of 1120rpm, 1400rpm and 80mm/min achieved the best strength and joint efficiency of 90%, due to the generated sufficient heat. Square pin profile produced higher strength joints compared to triangular and stepped profiles due to the four pulses per revolution. Placing AA2024 (harder alloy) on the advancing side (AS) improved the joint strength. Cole et al., [20] also noted that the material placed on the advancing side dominates a major portion of the weld zone.

A vertical milling machine was used to friction stir weld aluminium alloys 6035 and 8011 for evaluation of the mechanical properties in the dissimilar weld joint [21]. The welding parameters used were a constant rotational speed of 550rpm and varying welding speeds of 40-90mm/min. The tests performed to evaluate the FSW joint were the tensile tests, microstructural analysis and hardness tests. The more certifying results were at a welding speed of 60mm/min. The maximum tensile strength of 50MPa and maximum hardness of 91HV were obtained. The weld zone was divided into three regions (centre of weld, AA6035, AA8011) based on the microstructure. The centre of weld had fine grains due to dynamic recrystallization with higher tensile strength and hardness.

The dissimilar friction stir welding of undiluted copper and 1350 aluminium alloy sheet with a thickness of 3mm was investigated [22]. The AA1350 was placed on the advancing side of the tool. The welding parameters employed include a rotational speed of 1000rpm and a welding speed of 80mm/min. Microstructural analysis, hardness tests, tensile tests and SEM analysis were conducted. The microstructural results in the nugget zone showed the vortex-like pattern and lamella structure. There was no formation of IMCs in the nugget zone. The hardness dispersion revealed that the hardness on the copper side was higher than that on the AA side and the hardness at the bottom of the nugget was generally higher than those previously mentioned. The tensile properties of the dissimilar welds were UTS of 152MPa and elongation of 6.3%. A ductile-brittle mixed fracture surface was observed on the dissimilar joints of the tensile tested specimens.

The 6mm thick sheets of aluminium alloys 6061 and 5086 were friction stir welded together to analyse the evolution of microstructure in the stir zone and its influence on tensile properties of the joints [23]. The welding parameters used were the rotational speed of 500rpm, traverse speed of 35mm/min and the axial force of 4.9kN. The microstructure analysis, microhardness and tensile tests were conducted. The tensile properties of the joints correlated with microstructural features and microhardness values. The dissimilar joint exhibited a maximum hardness of 115HV and a joint efficiency of 56% which was higher than the hardness of the base metals. This was attributed to the defect-free stir zone formation and grain size strengthening.

2.2 TIG Welding of Dissimilar Alloys

One of the most important things to consider for TIG welding is the filler metal, which mainly depends on the alloys to be welded. Ishak et al., [24] investigated the welding of dissimilar aluminium alloys 6061 and 7075

using different filler metals namely ER4043 (Si-reach) and ER5356 (Mg–reach). The tests performed included visual appearance, microstructure and hardness tests. The results revealed that welding using filler ER5356 produced deeper penetration compared to filler ER4043. The use of ER5356 resulted in the depth of penetration of 1.74mm and 0.9mm of penetration attained using ER4043. Microstructures at different zones of dissimilar TIG joints such as the fusion zone, the PMZ and the HAZ were identified. The grain size (11.4μm) at fusion zone (FZ) for filler ER5356 specimens was finer than that of filler ER4043 which was 19.5μm. Average hardness values for filler ER5356 specimens were higher compared to filler ER4043 ones, which were 100HV and 86HV, respectively at HAZ of AA6061, 110HV and 88HV, respectively at FZ, while 113HV and 85HV, respectively at HAZ of AA7075. TIG welding using the ER5356 filler yielded better joint compared to ER4043.

The 12mm thick 5083 aluminium alloy was successfully TIG welded for the examination of the microstructure and mechanical properties on the welded joint [25]. A 12mm thick AA5083 plate and an ER536 filler wire were used. The results of the welded joint showed a fine and homogeneous microstructure when compared to the base metal. The microstructure in the HAZ was slightly coarsened compared to the microstructure in the weld. The tensile strength of welded joints was over 90% of that of 5083 base metal. The welded joint had high strength and ductility when compared to the base material ones.

TIG welding of dissimilar aluminium alloys is challenging due to the formation of brittle intermetallic compound (IMC). The IMCs have a negative effect on the joint's strength. Aluminium alloys 5083-H111 and 6061-T6 5mm thick plates were TIG welded using ER4047 filler rod [26]. Similar studies on TIG welding of 5083-O and 6061-T6 aluminium alloys were conducted by other researchers [27], [28], [29], [30] and [31]. The welding parameters used were a current of 200Amps, travel speed of 150mm/min and a voltage of 16V. The tests conducted included Vickers hardness, tensile tests and microstructural analysis. The results for the tensile properties of the welded joint were the UTS of 115MPa, percentage elongation of the welded joints of 3.09% and welded joint efficiency of 35.38%. The hardness value of the welded joint on the AA5083 side was more or less equal to the hardness value of AA5083, whereas, the hardness value on the AA6061 was above 120HV1. This was said to be due to the formation of the magnesium-silicon (Mg2Si) precipitates on the AA6061 side. The microstructural results showed elongated grains in the rolling direction. The microstructure of the weld joint was fairly coarser than the other two (AA5083 and AA6061). On the intersection, micropores and cavities were observed. The reduction in the ductility of the welded joint due to the presence of columnar grains is because of their anisotropic nature.

Narayanan et al., [32] TIG welded the aluminium alloy 5083. The welding parameters used were the welding currents of 200A and shielding gas flow rate of 15l/min. Various tests like tensile test; microhardness, macrostructure and microstructure study were conducted on the welded specimens. The test results showed the ultimate tensile strength of 281MPa, the hardness of weld metal of 73.5HVN. The obtained results were lower in comparison with the commercial mechanical properties of the AA5083 in which the UTS is 317MPa and hardness is 96HVN. In the heat affected zone precipitates were formed resulting in less elongation and increase in hardness, so the brittleness of material increased and the tensile strength of material decreased when compared to the base material.

A study on improving the welding quality of AA6031 plates using an automated TIG welding system was performed by Mohan, [33]. The welding parameters used were current of 180A, 50V voltage, welding speed ranged from 3.5-5mm/s, and a gas flow rate of 8-10l/min. The results showed a maximum tensile strength of 111.9MPa which was much lower than the tensile strength of the pure aluminium (90MPa). Additionally, the tensile strength of the weld joint was dependent on welding speed and welding current. The tensile strength value of the welded joint decreased from about 110MPa to 75MPa as the welding speed increased from 3.5mm/s to 5mm/s. The hardness value of the weld zone changed with the distance from weld centre due to change of the microstructure. For both sides, the welding tensile strength was found almost equivalent to the strength of base material.

TIG welding of 5083 and 6061 dissimilar aluminium alloy was conducted by Baghel & Nagesh, [34]. The thickness of the plates was 6.35mm. Tests performed included microstructure, tensile tests, microhardness, fractographs, and radiography to check porosities and lack of penetration. The results for the UTS of the weld joints were 213MPa, yield strength was 176MPa and elongation was 12%. Microstructural analysis results showed that both AA5083 and AA6061 undergone dynamic recrystallization. The higher and lower hardness results of 98HV and 72HV were attained at the fusion zone. The grain size increased as the welding speed increased. The fractographs results exhibited a dimple type rupture present at the surfaces due to insufficient or excessive heat which resulted in weaker weld integrity.

KumarSingh et al., [35] analysed the mechanical properties and microstructure of the AA5083 on the TIG welded joints. A constant current of 134A and gas flow rate of 7l/min were used during welding. The results revealed that tensile strength increased with the increase in welding speed but this linear relationship was noted until the speed of 100mm/min. Subsequently, after 100mm/min the tensile strength started to decrease as the welding speed continued to increase. The welding speed, current and gas flow rate were found to be very important parameters which were directly affecting the tensile strength of welded specimen and also plays an important role in metallurgical changes. The microstructure of the weld pool showed a refined grain size in comparison to the base metal.

TIG welding of dissimilar aluminium alloys 2014 and 5083 was successfully investigated by Sayer et al., [36]. One-sided TIG welding was applied with two passes. The welding parameters used were the Magmaweld TAL 4043 filler, current of 140A (root) – 150A (top), the voltage of 14V and argon gas flow rate of 10l/min. The tests performed included Vickers hardness, tensile tests and microstructural analysis. The microstructural analysis results in the weld region showed nonhomogeneous less equiaxed grain distribution with bigger diameters when compared to AA2014 and AA5083-O base metals. The grain size increase was said to be due to severe heat input. The tensile test results of the TIG AA2014 – AA5083 weld joint were a yield strength of 128MPa, UTS of 175MPa and elongation of 2.6%. The obtained values were lower than both BM values (42% and 74% for AA2014 and AA5083, respectively). The tensile test specimens fractured in the welded region. The SEM analysis revealed that a brittle fracture dominated the welds with the fracture zone located in the welded centre. The hardness resulted reported a sharp decrease of 84HV on the HAZ region of AA2014 side, due to severe heat input. Hardness increased in the weld region on the AA2014 side

followed by a decrease at the weld centre; due to the high Si content in the filler material. No significant decrease reported in the hardness on the HAZ region of AA5083.

Singh et al., [37] reported the mechanical properties of TIG welding at different parameters with and without the use of flux. The welding parameters used in the study included the welding current range of 105-140A, arc voltage of 16–18V, electrode diameter of 1.6–2.4mm and the gas flow rate of 8–10l/min. The results showed that the hardness (HRC) decreased from 65 to 60.2 (without flux), and from 58 to 52.5 (with flux) when the current increased from 105 to 140A. The results also showed that the increase in diameter of an electrode resulted in an increase in the hardness value. Additionally, the hardness of the weld joint was less in the case of welding without flux as compare to welding with flux.

AA7075-T651 and AA6061-T6 were TIG welded with the aim to investigate the hardness of the centre weld joint of the dissimilar aluminium alloys [38]. The welding parameters used were; Al-Si alloy filler wire with a diameter of 4mm, the flow rate of argon shield gas of 15l/min, the welding voltage of 80V, current of 280A, and the welding speed of 15mm/s. Brinell hardness tests and microstructural analysis tests were employed. The hardness recorded in the weld metal was 70.7BHN for the dissimilar joint. The voids presence in the TIG welds contributed to the reduced hardness of the joint.

2.3 Friction Stir Processing of Similar and Dissimilar Aluminium Alloys

The processing of dissimilar aluminium alloy 2024 and 6061 of 3mm thickness was accomplished using friction stir processing [39]. Mitsubishi CNC M70V milling machine was used for the application of FSW and FSP. Optimum welding parameters were used. The best results were obtained at the rotational speed 1800rpm and traverse speed of 25mm/min. Tensile tests, microstructural tests, residual stress analysis and X-ray tests were conducted. The results revealed the UTS efficiency of 77% and 71% for FSP and FSW respectively. The best microhardness value of 193.5HV was obtained across the weldment for FSP, and 139.8HV for FSW. The hardness of weld nugget was considerably higher than that of AA6061 base metal (BM) but comparatively lower than the AA2024 BM. FSW caused a decrease in the displacement density which resulted in a decrease of the microhardness. The FSP joint had a higher Vickers hardness value than the FSW joint because of FSP grain refinement and which was in agreement with the Hall-Petch relationship, which states that the hardness increases as the grain size decreases.

Karthikeyan and Kumar, [40] studied the relationship between process parameters and mechanical properties of a single pass friction stir processed 6063-T6 aluminium alloy plate. Processing was performed at different axial forces (8, 10 and 12KN), traverse speeds (22.2, 40.4 and 75mm/min) and tool rotational speeds (800, 1000, 12000, 14000 and 16000rpm). The results showed that at lower axial force FSP material exhibited lower tensile and ductility properties and on increasing the axial force, attained peak values but decreased with further increase. The specimens processed using an axial force of 10KN, tool feed of 40.2mm/min and a tool rotational speed of 1400rpm had an increase of about 46.5% in the tensile strength and ductility increased from 3% to 133%. The hardness followed the same trend as that of tensile properties.

Preprints (www.preprints.org) | NOT PEER-REVIEWED | Posted: 19 October 2019 doi:10.20944/preprints201910.0226.v1

Friction stir processing was applied on 6mm thick AA6056-T4 plates in order to break the large second phase particles into smaller and more resistant fragments [41]. Welding parameters used included a tool rotation rate of 500rpm and a traverse speed of 200mm/min. Microstructural analysis and tensile tests were performed on the FSP weld. The results showed that the intermetallic particle size decreases with the number of FSP passes. FSP was found to homogenize the particle distribution. Tensile test results revealed that the fracture strain of FSP samples was improved up to 90% in the best case compared to the base metal ones. Friction stir processing exhibited isotropy in fracture strain. From the results attained it was clear that FSP increased the ductility of the specimen compared to the base metal.

Mazaheri et al., [42] used the FSP technique to produce the A356/A2O3 surface composites. X-ray diffractometer, microstructural analysis, SEM, microhardness nanoindentation tests were used to characterize the samples. The microstructural analysis results of the A356/A2O3 indicated that A2O3 particles were well distributed in the aluminium matrix, and good bonding of the same alloy was generated. The FSP with A2O3 particles increased the microhardness of the substrates. The microhardness values for the dissimilar joint of A356–A2O3 and A356–nA2O3 surface composite were about 90 and 110HV, respectively. The hardness of the sample treated by the FSP without A2O3 particles and the as-received A356 were about 67 and 80HV, respectively. The results obtained from nanoindentation technique showed better microhardness and elastic modulus values for A356/A2O3 surface composites in comparison with as-received A356 and friction stir processed specimen (no A2O3).

Kalashnikova and Chumaevskii, [43] showed that friction stir processing can be used efficiently to the TiC particles distribution in aluminium based samples. A 2mm groove was prepared in the AA6082 plate in which reinforcement particles were dispersed using a tool. The process parameters employed were a tool rotational speed of 560rpm and traverse speed of 40mm/min. The mechanical properties improved after FSP due to modification in the microstructure. TiC particles significantly improved the microhardness and strengthened the composite. The highest hardness achieved was 73.5HV and was measured on the zone with the accumulated additional TiC particles.

The effect of FSP on AA2024-T3 was studied by Hashim et al., [44]. A 5mm thick, 250mm long and 100mm wide plate was used. A vertical milling machine was used for the friction stir processing of the plate. The process parameters used included the flat pinless cylindrical shoulder of 10mm, rotational speed of 945rpm and a traverse speed of 85mm/min. Tensile tests, microstructure analysis and hardness tests were conducted. FSP resulted in an increase in hardness of the processed joint compared to the base material. An increase in yield strength, percentage elongation and UTS compared to those of the base material was noted. The microstructure grain size refinement correlated with the tensile and hardness test results.

The cast Al-Si base alloy was subjected to friction stir processing for the analysis of mechanical properties [45]. The tensile properties of cast AC8A alloy were improved after FSP, particularly the tensile elongation, which increased from < 1% to 15.4%. FSP resulted in improvement of the tensile strength as the result of a combination of dissolution, coarsening and strengthening precipitates, which were attained by the FSP parameters. Jana et al., [46] investigated the FSP effect on fatigue behaviour of the cast Al–7Si–0.6 Mg alloy.

The results showed five times improvement in fatigue life for a hypoeutectic Al–Si–Mg cast alloy. FSP eliminated the porosities and refined the Si particles resulting in a decrease of the crack growth rate. In addition, FSP resulted in both break-ups of the dendritic microstructure and complex material mixing.

Kurt et al., [47] performed FSP on the aluminium alloy 1050 to improve respective mechanical properties. Samples were subjected to the various tool rotating and traverse rates with and without SiC powders. The optimum processing parameters that were found to give better results were the rotational speed of 1000rpm and traverse speed of 20mm/min. The results revealed that FSP decreased the grain size and increased the hardness of processed material. A good dispersion of SiCp was obtained for the composite layer. The hardness of created composite surfaces was improved by a multiple times when compared with that of base metal. Bending strength of the produced metal matrix composite was significantly higher than processed plain specimen and untreated base metal. The high microhardness of Al/SiCp composite attributed to the presence of reinforcement particles, which also improved the bending strength.

AA2014 aluminium alloy with a thickness of 3mm was subjected to FSP using a tool made up of Cr–Mo steel [48]. The recommended operating parameters were a tool speed of 1000rpm, traverse feed rate of 60mm/min and 2° tilt angle. Five different tool pin profiles were tested and the hexagonal tool possessed the highest UTS of 398MPa and yield tensile strength of 365MPa. The highest hardness value found in the nugget zone for hexagonal processed tool pin was 148.6HV. The microstructural study confirmed that the sample processed with hexagonal tool exhibited superior surface properties compared to the rest of the tools. FSP resulted in grain refinement from 87.5μ to 2.5μ. The SEM results revealed that the grain size at the nugget zone exhibited reduction in granular volume of α-aluminium phase, which lead to the enrichment of hardness. This exceptional quality of grain refinement improved the overall structural stability and integrity of the material.

The influence of FSP on the microstructure and mechanical properties in terms of hardness for AA6061 sheet was studied and investigated [49]. The workpiece was subjected to FSP by different number of passes utilizing cylindrical shaped geometry type high steel tool. Microstructural evaluation of the modified surfaces was carried out using optical microscopy. From the microstructural evaluation, the grain size of the processed area decreased by 70% compared to the unprocessed base metal. This was anticipated due to grain refinement by the FSP tool in the material during processing. The hardness results indicated that as the number of passes increased, the hardness of the produced composite surfaces increased steadily. It was noted here that the strength of stirred surface area was 1.75 times higher than the unstirred surface area.

The 7039 aluminium alloy was friction stir processed for the analysis of mechanical properties compared to the base material ones [50]. The modified surfaces were characterized in respect to macrostructure, microstructure, hardness and tensile properties. The results showed an increase in ductility from about 13.5% to 23.6% while the ultimate and yield strength were adversely affected. The results showed higher ductility on the longitudinal direction than in traverse direction. The multi-pass friction stir processing produced higher hardness than the single pass one. The friction stir processed AA7039 hardness test results were found to be lower than that of the unprocessed alloy.

Santella et al. [51] showed that FSP created a uniform distribution of broken second-phase particles of A319 and A356 and eliminated the coarse and heterogeneous structure of the alloys. The study was performed to assess the mechanical properties and reported that the tensile and fatigue behaviour of the material were improved with friction stir technique. The TEM observations revealed the generation of a fine-grained structure of 5 to 8μ in FSP A356. Furthermore, TEM examinations revealed that the coarse Mg2Si precipitates in the as-cast A356 sample disappeared after FSP, indicating the dissolution of most of the Mg2Si precipitates during FSP. After FSP, most of the solutes were retained in solution, due to rapid cooling from the FSP temperature, thereby forming a supersaturated aluminium solid solution.

Wrought aluminium alloy 5059 with a 6.3mm thickness was friction stir processed using 3 different tool shapes, and 3 different rotation speeds [52]. The tests employed include microstructural analysis microhardness and tensile tests. Preliminary results indicated that a fine grained structure was achieved with improved mechanical properties. The results showed that FSP with a rotation speed of 638 RPM using a tool with a 3-flat threaded pin produced an average grain size of 1.24μm in the stir zone. Applying higher rotation speeds, or use of tools with a conventional threaded or grooved pin which did not contain flats resulted in larger grains. The tensile properties attained were a yield strength of 250MPa and UTS of 357MPa were slightly higher than those of the as-received material, while the elongation at fracture was significantly improved up to 26%. The tensile results correlated with the grain refinement occurred as a result of dynamic recrystallization during FSP.

Friction stir processing of cast Mg–9Al–1Zn alloy plus subsequent aging produced a defect-free recrystallized fine-grained microstructure with fine β-Mg17Al12 particles [53]. Compared to the as-cast parent material, the FSP sample exhibited significantly enhanced fatigue properties, with the fatigue strength being increased from 45 to 95MPa and the fracture mode being changed from quasi-cleavage fracture to dimple fracture. The improvement was attributed to the refinement of grains, elimination of porosities and coarse β networks, and precipitation of fine β particles.

Sakurada et al., [54] were the first to perform a study on underwater friction joining process. Their study was utilising the 6061 aluminium alloy. Their results showed that it was possible to generate enough friction for processing even though the workpieces were underwater. The stirred region of the underwater weld joint showed a finer microstructure in comparison to the one exposed to room temperature air conditions. The elongation of the underwater joints was lower than that of the air. The results also revealed the hardness increase in AA6061 from 60 to 90HV which lead to a joint efficiency increase of 33%. Hofmann & Vecchio, [55] studied the effect of submerging FSP on the grain size of Aluminum alloy Al-6061-T6 compared to in air FSP. Their results showed that more grain refinement was attained under submerging conditions due to a faster cooling rate. They also used boundary migration model to predict the grain size using measured thermal histories of the stirred material.

The fracture of the underwater joints was discovered to be dependent on the tool rotational speed [56]. The joints welded at 600, 800 and 1000-1200rpm were tensile fractured in the SZ, TMAZ and HAZ respectively. Darras & Kishta [57] investigated the friction stir processing of AZ31 magnesium alloy in normal and

submerged conditions and their effect on tensile properties, grain structure, power consumption, and thermal fields. The average grain size of 18.9µm, 15.9µm, and 13.3µm were obtained for FSP in the air, submerged in hot water and cold water respectively. The most grain refinement was found in cold water FSP conditions. The thermal results revealed the peak temperature for weld in air as highest at 477K as in the case of cold and hot water joint, it was 385K and 433K respectively. The time spent for the processing is 16.5s, 7s and 4s for FSP in the air, submerged in hot water and cold water. From the results it was evident that SFSP not only reduces the temperature but also reduce the time spent processing the material. Sabari et al. [58] reported that the higher temperature gradient (along transverse and longitudinal weld axes) and higher cooling rate in underwater friction stir welds were a result of uniform heat absorption capacity of water when compared to the air-cooled welds.

Commercial 5083 aluminium alloy rolled plates were subjected to friction stir processing (FSP) with a tool rotational speed of 430rpm and a traverse feed rate of 90mm/min [59]. The microstructure analysis showed a fine grain of 1.6µm and an average disorientation angle of 24º. Ductility was measured using tensile elongations at a temperature of 250ºC at three strain rates, and demonstrated that a decrease in grain size resulted in significantly enhanced ductility and lower forming loads. The ductility of the friction stir processed material was enhanced by a factor ranging from 2.6 to 5 compared to the ductility of the base metal, in the range of the strain rates tested. The strain rate sensitivity of the processed material was 0.33 while for the base metal was 0.018. The deformation mechanism in the fine-grained specimens was mainly controlled by solute drag creep, though the contribution of grain boundary sliding to the deformation process cannot be overlooked. Both mechanisms led to significant flow localization and simultaneous cavity formation.

Akinlabi et al., [60] showed the effect of the tool rotational and traverse speeds as well as the number of passes on tribological characteristics of the modified surfaces was investigated. The FS-processed samples exhibited lower wear rates than the as-cast A390 hypereutectic Al–Si alloy. The wear rates were found to be reduced by reducing the tool rotational speed and increasing the tool traverse speed. Increasing the number of FSP passes reduced the wear rate as well as the coefficient of friction. While the minimum average coefficient of friction was about 0.33 for samples Friction Stir-processed for three pass at 1200rpm and 20mm/min. The wear resistance of the FS-processed samples was improved by increasing the tool traverse speed and reducing the tool rotational speed.

Toma et al., [61] proved that the FSP tool cutting depth has an effect on the mechanical properties and microstructures of aluminium alloy 6061-T6. Friction stir process tool travel and rotation speeds effects on the surface topography, hardness, tensile mechanical properties and microstructures of aluminium alloy were studied. The cylindrical tool without pin diameter (20 mm), tool rotational speed (800 rpm) and travel speed (60 rpm) employed. The test results indicated that the hardness increased with the cutting depth. The crystal structure analysis revealed that the hardness increased in the case of two stages twice the case of one stage. It was also noted that the size of the engineering flaws granules became smaller and the size of these granules increased with the cutting depth. In addition, the ratio of granule size and the friction in the case of two stages was twice the case of one stage.

Abrahams et al., [62] investigated the properties and microstructure of friction stir processed 7075-T651 aluminium alloy using various tool designs. Trials were conducted on AA 5005-H34 with the aim of determining the most suitable FSP tool design out of the considered three different pin designs. Fully recrystallized fine microstructure and a defect free processed zone were achieved through the use of some of the FSP pin designs. FSP application resulted in grain refinement of the processed zone of AA5005-H34. The grain sizes were refined from the initial 192µm pancake-like microstructure in the AA 5005-H34 base material to 10–20µm in the processed regions. Similarly, on the AA7075-T651 the grain size of the base metal decreased from 50µm to 4–10µm in the processed regions of the FSP of the same aluminium alloy. The traverse speed had a greater influence on the microhardness and mechanical properties, compared to the tool rotational speed. Microhardness and mechanical properties were improved as the traverse speed increased, due to the reduction in the precipitate-free zones at the grain boundaries.

Effect of the processing parameters of friction stir processing on the microstructure and mechanical properties of 6063 aluminium alloy was added to the literature [63]. After FSP, fine equiaxed α-Al grains formed in the weld nugget of 6063 Al alloy, and their size increased with increasing tool rotation speed in the range of 300–700rpm. Tunnel defects were observed in the TMAZ for a low tool rotation speed of 300rpm. When the rotational speed exceeded 700rpm, a good combination interface can form between the WN and the TMAZ. Electron backscatter diffraction results showed that the fraction of the high-angle grain boundary was increased after FSP in the WN. The alloys exhibited a more concentrated distribution and higher densities. The TEM analysis results showed that the densities of needle-shaped precipitates were reduced in the WN. Some high-density dislocation pile-ups formed at some grains. The UTSs was lower than that of the base metal at lower tool rotation speeds. With increasing speed, the UTSs increased gradually and then became higher than that of the BM. The strain values were all lower than that of the BM.

The 5mm thick sheets of AA7075 were subjected to underwater and room temperature friction stir technique for the analysis of metallurgical and mechanical properties [64]. The variable process parameters were used. The temperature during FSP was monitored and recorded using the K-type thermocouple placed underneath the plate close to the abutting line of the workpiece. The average grain and precipitate sizes of the weld nugget zones were significantly reduced by the submerged conditions and travel speed increase. A critical travel speed of 150mm/min was attained in underwater welds beyond which the average grain sizes remain relatively the same. Optimum weld strengths of 396 and 360MPa were obtained in the underwater and air-cooled welds at tool rotational and travel speeds of 800rpm and 50mm/min respectively.

Fabrication of the AA6063/SiC composite material by doping SiC via friction stir processing [65]. The selected material was friction stir processed at constant tool rotational and welding speed of 1400rpm and 65mm/min respectively. SiC particles were incapacitated in a series of holes of 2mm diameter and 4.8mm depth made in AA6063 plate for the fabrication of composite. Tests conducted include tensile, impact, microhardness, and microstructure testing. The results for microhardness of the stir zone of fabricated AA6063/SiC composite has high microhardness (95HV) as compared to the base material. The increase in hardness was due to the presence and pining effect of hard SiC particles. Fabricated AA6063/SiC composite material had a high

tensile strength at the rate of 220MPa as compared to the base metal. The increase in tensile strength and the formation of fine grain structure was beacause of the good bonding between SiC particles and base metal.

The microstructural modification of AA206 through the use of FSP was also reported in the literature [66]. This modification was performed so as to comparatively evaluate the mechanical properties of processed and unprocessed AA206 material. A 6.26mm and 16mm thick plates were used for tensile and fatigue test respectively. The two key processing parameters were tool rotation speed of 1000rpm and tool traverse speed of 50.8mm/min. The results showed an increase in both yield strength and UTS after FSP when compared to those of the base metal. There was a notable improvement in yield strength and UTS on the processed plates compared to the base material. The percentage of elongation and fatigue strength also increased compared to the unprocessed ones. The increase in these properties correlated with the grain size refinement and homogeneity.

Thakral et al., [67] used FSP to enhance the tensile properties and hardness of the TIG welded AA6061-T6 joint. The tests performed include tensile, hardness and microstructure analysis. Tensile results showed that the average UTS value for the base metal was 299MPa, 85MPa for the TIG weld joint and 125MPa for FSP TIG joint. An increase of 48% was reported on the UTS on the TIG welded joint. The hardness values of FSP TIG specimen ranged from 72-74HV which was almost similar to that of base metal which was 74HV whereas in TIG specimen hardness value ranged from 66-68HV. Microstructural analysis was performed on the weld zone to evaluate the effect of welding parameters on welding quality and grain structure. The microstructure of FSP TIG joint showed very fine equiaxed recrystallized grains compared to the microstructure of TIG joint. This, therefore, meant that FSP can be used as a post-processing technique.

The effect of a single pass FSP on the mechanical properties and microstructure of the commercially pure aluminium was investigated [68]. The parameters employed were a downward force of 5kN, traverse speed of 150mm/min and the tool rotation speed of 640rpm. FSP resulted in refined grain size of 3µm from the base metal grain size of 84µm. The TEM results presented fine grains with well-defined boundaries. The tensile results showed UTS increase of 25% from 72 to 90MPa and the ductility decreased by about 10%. The impurity particles observed in TEM resulted in the yield strength of 35MPa. The hardness also improved substantially from 29HV to 42HV.

Feng et al., [69] investigated the effect of SFSP on the microstructure of the 2.5mm thick aluminium alloy 2219 sheet. Process parameters used were the traverse speed of 200mm/min and rotational speeds ranging from 600 to 1000rpm. Tests employed include microstructure analysis, microhardness. The grain size on the stir zone was less than that of the base metal. The area fraction of the ultra-fine grains in the stir zone increased as heat input decreased. The results showed a decrease in microhardness of the SFSP stir zone compared to that of the unprocessed BM. The exhibited average microhardness in the stir zone were 95HV and 100HV, corresponding to the tool rotational speed of 1000rpm and 800rpm

The 6mm thick aluminium alloy 6082 was subjected to underwater FSP to test the changes in the UTS [70]. The High Carbon High Chromium Steel rod of diameter 20mm material was used as the processing tool for

this investigation. The result revealed that the maximum tensile strength of the underwater joints was higher (221.6MPa) than that of the normal air (195MPa).

The effect of SFSP on the mechanical and microstructural properties of 10mm thick AA7075 was investigated [71]. A thermocouple was used to record the temperature of water. The FSP caused the non-uniform structure of the raw material with an average grain size of 18 micrometers to change into a uniform structure. The single pass FSP was carried out using a traverse speed of 40 and 63mm/min and a rotational speed of 800 and 1250rpm in the water and at the ambient temperature. 1250rpm and 63mm/min were found to be the optimum rotational and traverse speed respectively. Tests conducted include macro and micro Structure analysis, microhardness, and tensile tests. The microstructural results revealed that FSP refined the structure to the grain size to 8.2µ for underwater and 12.1µ for air. Tensile results showed an improvement in yield stress, ultimate stress, and elongation of the specimens after FSP. 115MPa, 405MPa, 33.5% respectively for underwater. For FSP in the air, the results were yield strength of 117MPa, UTS of 405MPa and 28.5% for elongation. Furthermore, Vickers average hardness results 148HV in the water and 131HV in the air, showing a decrease compared to the BM which was 156HV.

2.4 Mostly Processed Welding Techniques

Based on the literature cited the most friction stir processing is done on the to enhance the properties of the base metal rather than welded joints. Few literatures [39, 52] reports on post processing the friction stir welded joints, while only [68] reports on using FSP as a post processing of the TIG welded joints. No other searchable literature obtained on post processing for both FSW and TIG welded joints.

2.5 Mostly Processed Grades

The most processed aluminium alloy series based on the presented literature was 6xxx (6061, 6082, 6063, 60560), with 6061 taking a lead. Following the 6xxx was the 7xxx (7075, 7039), 2xxx (2024, 2219, 2014) and the 5xxx (5005, 5083, 5059).

3 Conclusions

In all the work that has been performed thus far, it has been noted that all the focus has been on FSP as an enhancement technique on aluminium alloys, magnesium and other alloys. It is also noticed that the common mechanical properties analysed include the tensile test, fatigue and microhardness. These properties are studied correlatively with the microstructure. No literature has been reported so far, which considers FSP as a post weld processing technique for TIG dissimilar alloy welded joint. There is also no trace of any literature on submerged friction stir processing of TIG and FSW welded dissimilar alloy joints. The therefore opens a gap on the FSP and SFSP as a post-processing technique to the dissimilar alloy weld joints for FSW and TIG welding techniques.

 doi:10.20944/preprints201910.0226.v1

Supplementary Materials

There is no supplementary material for this manuscript.

Acknowledgements

The authors would like to thank the Cape Peninsula University of Technology for allowing us to pursue this study.

Author Contributions

Both authors have fully contributed equally to all the work produced.

Conflict of Interest

The authors would declare no conflict of interest. The authors declare there is no funding involved in this study.

References

1. Cam G.; Kocak M. Progress in joining of advanced materials. *Int. Mater. Rev* **1998**, 43, 1–44.

2. Nicholas E.D. ICAA-6 Aluminium Alloys Proceedings, Cambridge, UK, 1998, v. 1, pp. 139–51.

3. Patel V.; Li W.; Wang G.; Wang F.; Vairis A.; Niu P. Friction stir welding of dissimilar aluminum alloy combinations: State-of-the-art. *Metals* **2019**, 9(3), 270, 1-19.

4. Sun N. Friction Stir Processing of Aluminium Alloys. Master of Science Thesis. Lexington, Kentucky, 2009.

5. Marczyk J.; Nosal P.; Hebda M. Effect of Friction Stir Processing On Microstructure and Microhardness of Al – Tic Composites. Student's conference, Czech Technical University in Prague, Faculty of Mechanical Engineering, Freiberg Deutschland, 8-9 November 2018.

6. Węglowski M.S. Friction stir processing – state of the art. *Arch. Civil and Mech. Eng.* **2018**, 18, 114-129.

7. Chaudhari R.; Parekh R.; Ingle A.; Reliability of Dissimilar Metal Joints Using Fusion Welding: A Review. International Conference on Machine Learning, Electrical and Mechanical Engineering (ICMLEME'2014) Dubai Jan. 8-9, 2014.

8. Simar A.; Joncheere C.; Deplus K.; Pardoen T.; de Meester B. Comparing similar and dissimilar friction stir welds of 2017–6005A aluminium alloys. *Sci. and Technol. of Welding and Joining* **2013**, 15(3), 254–259.

9. Dilip J.J.S.; Koilraj M.; Sundareswaran V.; Janaki Ram G.D.; Koteswara Rao S.R. Microstructural characterization of dissimilar friction stir welds between AA2219 and AA5083. *Trans Indian Inst. of Met*. **2010**, 63(4), 757–764.

10. Taiki M.; Atsushi K.; Masato T.; Makoto H.; Tomotake H.; Kenji H. Dissimilar welding of Al and Mg alloys by FSW. *Mater. Trans.* **2008**, 49(5), 1129–1131.

11. Cavaliere P.; Panella F. Effect of tool position on the fatigue properties of dissimilar 2024-7075 sheets joined by friction stir welding. *J. Mater. Process. Technol.* **2008**, 206(1–3), 249–255.

12. Peng G.; Yan Q.; Hu J.; Chen P.; Chen Z.; Zhang T. Effect of forced air cooling on the microstructures, tensile strength, and hardness distribution of dissimilar friction stir welded AA5A06-AA6061 joints. *Met.* **2019**, 9(304), 1-10.

13. Upadhyay P.; Reynolds A.P. Effects of thermal boundary conditions in friction stir welded AA7050-T7 sheets. *Mater. Sci. Eng. A.* **2010**, 527(6), 1537–1543.

14. Giraud L.; Robea H.; Claudina C.; Desrayaud C.; Bocherd P.; Feulvarcha E. Investigation into the dissimilar friction stir welding of AA7020-T651 and AA6060-T6. *J. Mater. Process. Technol.* **2016**, 235, 220–230.

15. Khodir S.A.; Shibayanagi T. Dissimilar friction stir welded joints between 2024-T3 aluminum alloy and AZ31 magnesium alloy. *Mater. Trans.* **2007**, 48(9), 2501–2505.

16. Rodriguez R.I.; Jordon J.B.; Allison P.G.; Rushing T.; Garcia L. Microstructure and mechanical properties of dissimilar friction stir welding of 6061-To-7050 aluminum alloys. *Mater. Des.* **2015**, 83, 60–65.

17. Guo J.F.; Chen H.C.; Sun C.N.; Bi G.; Sun Z.; Wei J. Friction stir welding of dissimilar materials between AA6061 and AA7075 Al alloys effects of process parameters. *Mater. Des.* **2014**, 56, 185-192.

18. Mofid M.A.; Abdollah-Zadeh A.; Gürza C.H. Investigating the formation of intermetallic compounds during friction stir welding of magnesium alloy to aluminum alloy in air and under liquid nitrogen. *Int. J. Adv. Manuf. Tech.* **2014**, 71(5–8),1493–1499.

19. El-Hafez H.A.; El-Megharbel A. Friction stir welding: Dissimilar Aluminum Alloys. *World J. Eng. and Technol.* **2018**, 6, 408-419.

20. Cole E.G. Weld temperature effects during friction stir welding of dissimilar aluminum alloys 6061-T6 and 7075-T6. *Int. J. Adv. Manuf. Tech.* **2014**, 71(1–4), 643–652.

21. Vivekanandan P.; Arunachalam V.P.; Prakash T.; Savadamuthu L. The experimental analysis of friction stir welding on aluminium composites. *Int. J. Metallur. Eng.* **2012,** 1(4), 1–6.

22. Li X.; Zhang D.; Qiu C.; Zhang W. Microstructure and mechanical properties of dissimilar pure copper / 1350 aluminum alloy butt joints by friction stir welding. *Trans. of Nonfer. Meta. Society of China*, **2012**, 22(6), 1298–1306.

23. Ilangovan M.; Boopathy S.R.; Balasubramanian V. Microstructure and tensile properties of friction stir welded dissimilar AA6061-AA5086 aluminium alloy joints. *Trans. of Nonfer. Meta. Society of China (English Ed.)*, **2015**, 25(4),1080–1090.

24. Ishak M.; Mohd Noordin N. F.; Ahmad Shah L. H. Feasibility study on joining dissimilar aluminum alloys AA6061 and AA7075 by tungsten inert gas (TIG). J. *Teknol.* **2015**, 75(7), 79–84.

25. Xuebao H. Microstructure and mechanical properties of 5083 aluminum alloy joint by TIG welding. *Trans. China Welding Inst.* **2014**, 35(1), 37-40.

26. Waleed W.A.; Subbaiah K. Effect of ER4047 filler rod on tungsten inert gas welding of AA5083-H111 and AA6061-T6 aluminium alloys. *JCHPS* **2017**, (7), 210–213.

27. Sefika K. Multi-response optimization using the Taguchi based grey relational analysis: a case study for dissimilar friction stir butt welding of AA6082-T6/AA5754-H111, *Int. J. Adv. Manuf. Technol.* **2013**, 68, 795-804.

28. Subbaiah K.; Geetha M.; Sridhar N.; Koteswara Rao S.R. Comparison of tungsten inert gas and friction stir welding of AA 5083- H321 aluminium alloy plates. Trends in Welding Research, Proceeding of the 9th International Conference, ASM International, Chicago, Illinois, USA, 4-8 June 2012.

29. Leitao C.; Louro R.; Rodrigues D.M. Analysis of high temperature plastic behavior and its relation with weld ability in friction stir welding for aluminum alloys AA5083-H111 and AA6082-T6. *Mater. Des.* **2012**, 37, 402-409.

30. Menzemer C.C.; Lam P.C.; Wittell C.F.; Srivarsan T.S. A study of fusion zone microstructures of arc-welded joints made from dissimilar aluminum alloys. *J. Mater. Eng. Perf*. **2001**, 10 (2), 173-178.

31. Palanivel R.; Koshy Mathews P.; Murugan N. Optimization of process parameters to maximize ultimate tensile strength of friction stir welded dissimilar aluminum alloys using response surface methodology. *J. Cent. South Uni.* **2013**, 20, 2929-2938.

32. Narayanan A.; Mathew C.; Baby V.Y.; Joseph J. Influence of gas tungsten arc welding parameters in aluminium 5083 alloy. *IJESIT* **2013**, 2(5), 269–277.

33. Mohan P. Study The Effects of Welding Parameters on TIG Welding of Aluminum Plate. Master of Technology in Production Engineering, National Institute of Technology, Rourkela, India, 2014.

34. Baghel P.K.; Nagesh D.S. Mechanical properties and microstructural characterization of automated pulse TIG welding of dissimilar aluminum alloy. *IJEMS* **2018**, 25(April), 147–154.

35. KumarSingh S.; Tiwari R.M.; Kumar A.; Kumar S.; Murtaza Q.; Kumar S. Mechanical Properties and Microstructure of Al-5083 by TIG. International Conference on Processing of Materials, Minerals and Energy 2018, Ongole, Andhra Pradesh, India, July 29th – 30th.

36. Sayer S.; Yeni C.; Ertugrul O. Comparison of mechanical and microstructural behaviors of tungsten inert gas welded and friction stir welded dissimilar aluminum alloys AA 2014 and AA 5083. *Meta Mater.* **2011**, 49(2), 155–162.

37. Singh G.; Singh F.; Singh H. A Study of mechanical properties on TIG welding at different parameters with and without use of flux. *IJTIR* **2015**, 16(July), 2321–1814.

38. Patil C.; Patil H.; Patil H. Experimental investigation of hardness of FSW and TIG joints of aluminium alloys of AA7075 and AA6061. *Frattura Integr. Strutt.* **2016**, 10(37), 325–332.

39. Hameed A.M.; Resan K.K.; Eweed K.M. Effect of friction stir processing parameters on the dissimilar aluminum alloys. ASME International Mechanical Engineering Congress and Exposition 2015, Houston, Texas, November 13-19.

40. Karthikeyan L.; Kumar V.S. Relationship between process parameters and mechanical properties of friction stir processed AA6063-T6 aluminum alloy. *Mater. Des.* **2011**, 32(5), 3085–3091.

41. Hannard F.; Castin E.; Pardoen T.; Mokso T.; Maire E.; Simar A. Ductilization of aluminium alloy 6056 by friction stir processing. Institute of Mechanics, Materials and Civil Engineering, Université catholique de Louvain, 2017, 1–3.

42. Mazaheri Y.; Karimzadeh F.; Enayati M.H. A novel technique for development of A356/Al2O3 surface nanocomposite by friction stir processing. *J. Mater. Process. Technol.* **2011**, 211(10), 1614–1619.

43. Kalashnikova T.A.; Chumaevskii A.V.; Rubtsov V.E.; Ivanov A.N.; Alibatyro A.A.; Kalashnikov K.N. Structural evolution of multiple friction stir processed AA2024. International Conference on Advanced Materials with Hierarchical Structure for New Technologies and Reliable Structures 2017 (AMHS'17), Tomsk, Russia, 9–13 October 2017.

44. Hashim F.A.; Salim R.K.; Khudair B.H. Effect of friction stir processing on (2024-T3) aluminum alloy. *IJIRSET* **2015**, 4(4), 1822–1829.

45. Tsai F.; Kao P. Improvement of mechanical properties of a cast Al-Si base alloy by friction stir processing, *Mater. Lett.* **2012**, 80, 40-42.

46. Jana S.; Mishra R.; Baumann J. Effect of friction stir processing on fatigue behavior of an investment cast Al–7Si–0.6 Mg alloy. *Acta Mater.* **2010**, 58(3), 989–1003.

47. Kurt A.; Uygur I.; Cete E. Surface modification of aluminium by friction stir processing. *J. Mater. Process. Technol*. **2010**, 211(3), 313–317.

48. John J.; Shanmuganatan S.P.; Kiran M.B.; Senthil Kumar V.S.; Krishnamurthy R. Investigation of friction stir processing effect on AA 2014-T6. *Mater. Manuf. Process* **2019**, 34(2), 159–176.

49. Prakash T.; Sasikumar P. The Influences of the friction stir processing on the microstructure and hardness of AA6061 aluminium sheet metal. *JMET* **2013**, 1(1), 66–72.

50. Sinhmar S.; Dwivedi, D.K.; Pancholi V. Friction stir processing of AA 7039 alloy. International Conference on Production and Mechanical Engineering 2014, Bangkok, Thailand, December 30-31.

51. Santella M.L.; Engstrom T.; Storjohann D.; Pan T.Y. Effects of friction stir processing on mechanical properties of the cast aluminum alloys A319 and A356. *Scr. Mater.* **2005**, 53, 201–206.

52. Izadi H.; Nolting A.; Munro C.; Gerlich A.P. Effect of friction stir processing parameters on microstructure and mechanical properties of AL 5059. Trends in Welding Research, Proceedings of the 9th International Conference, Chicago, Illinois, USA, 2012 June 4-8.

53. Ni D.R.; Wang D.; Feng A.H.; Yao G.; Ma Z. Enhancing the high-cycle fatigue strength of Mg–9Al–1Zn casting by friction stir processing. *Scr. Mater.* **2009**, 61(6), 568–571.

54. Sakurada D.; Katoh K.; Tokisue H. Underwater Friction welding of 6061 aluminum alloy. *JILM* **2002**, 52(1), 2–6.

55. Hofmann D.C.; Vecchio K.S. Thermal history analysis of friction stir processed and submerged friction stir processed aluminum. *MSEA* **2007**, 465(1–2), 165–175.

56. Zhang H.J.; Liu H.J.; Yu L. Microstructure and mechanical properties as a function of rotation speed in underwater friction stir welded aluminum alloy joints. *Mater. Des.* **2011**, 32(8-9), 4402-4407.

57. Darras B.; Kishta E. Submerged friction stir processing of AZ31 Magnesium alloy. *Mater. Des.* **2013**, 47, 133–137.

58. Sabari S.S. Evaluation of Performance of Friction Stir Welded AA2519-T87 Aluminium Alloy Joints. Doctor of Philosophy in Manufacturing Engineering, Annamalai University, Tamil Nadu, India, 01 September 2016.

59. El-Danaf E.A.; El-Rayes M.M.; Soliman M.S. Friction stir processing: an effective technique to refine grain structure and enhance ductility. *Mater. Des.* **2010**, 31(3), 1231–1236.

60. Akinlabi E.T.; Mahamood R.M.; Akinlabi S.A.; Ogunmuyiwa E. Processing parameters influence on wear resistance behaviour of friction stir processed Al-TiC composites. *Adv. Mater. Sci. Eng*. **2014**, 1-12.

61. Toma E.; Karash B.Y.; Saeed R.; Taqi M.; Qasim E. The effect of the cutting depth of the tool friction stir process on the mechanical properties and microstructures of aluminium alloy 6061-T6. *AJMA* **2015**, 3(5), 33-41.

62. Abrahams R.; Mikhail J.; Fasihi P. Effect of friction stir process parameters on the mechanical properties of 5005-H34 and 7075-T651 aluminium alloys. *Mater. Sci. Eng.* **2019**, 751, 363–373.

63. Zhao H.; Pan Q.; Qin Q.; Wu Y.; Su X. Effect of the processing parameters of friction stir processing on the microstructure and mechanical properties of 6063 aluminum alloy, Mater. Sci. Eng. **2019**, 751, 70–79.

64. Rouzbehani R.; Kokabi A.H.; Sabet H.; Paidar M.; Ojo O.O. Metallurgical and mechanical properties of underwater friction stir welds of Al7075 aluminum alloy. *J. Mater. Process. Technol.* **2018**, 262, 239–256.

65. Singh I.; Singh T.; Singh R.; Singh S.G. Fabrication of AA-6063/Sic composite material by using friction stir processing. *IJAR* **2017**, 5(4),1652–1656.

66. Sun N.; Jones W. J.; Apelian D. Friction stir processing of aluminum alloy A206: Part II—tensile and fatigue properties. *Int. J. Metalcast* **2019**, 13(2), 244–254.

67. Thakral R.; Sanjeev S.; Taljeet S. Experimental analysis of friction stir processing of TIG welded aluminium alloy 6061. *IJIRST* **2018**, 4(8), 51–57.

68. Yadav D., Bauri R. Effect of friction stir processing on microstructure and mechanical properties of aluminium. *MSEA*. **2012**, 539(March), 85–92.

69. Feng X.; Liu H.; Lippold J.C. Microstructure characterization of the stir zone of submerged friction stir processed aluminum alloy 2219. *Mater. Charact.* **2013**, 82, 97–102.

70. Singh H.; Kumar P.; Singh B. Effect of under surface cooling on tensile strength of friction stir processed aluminium alloy 6082. *AJEAT* **2016**, 5(1), 40–44.

71. Nourbakhsh S. H.; Atrian A. Effect of submerged multi-pass friction stir process on the mechanical and microstructural properties of Al7075. *J. Stress Anal* **2017**, 2(1), 51–56.